Measurement of Shear and Slip with a GelSight Tactile Sensor

Wenzhen Yuan[1], Rui Li[2], Mandayam A. Srinivasan[3] and Edward H. Adelson[4]

Abstract— **Artificial tactile sensing is still underdeveloped, especially in sensing shear and slip on a contact surface. For a robot hand to manually explore the environment or perform a manipulation task such as grasping, sensing of shear forces and detecting incipient slip is important. In this paper, we introduce a method of sensing the normal, shear and torsional load on the contact surface with a GelSight tactile sensor [1]. In addition, we demonstrate the detection of incipient slip. The method consists of inferring the state of the contact interface based on analysis of the sequence of images of GelSights elastomer medium, whose deformation under the external load indicates the conditions of contact. Results with a robot gripper like experimental setup show that the method is effective in detecting interactions with an object during stable grasp as well as at incipient slip. The method is also applicable to other optical based tactile sensors.**

I. INTRODUCTION

Tactile sensing is an important aspect of sensation and perception for both humans and robots, because it conveys a great deal of information about the interaction of the body with the environment. Comprehensive reviews of artificial tactile sensing are given in [2] and [3]. Although several successful commercial tactile sensors have been developed (e.g., [4] and [5]), significant limitations exist in currently available robotic tactile sensors. There is a great need for their continued development, particularly for sensing shear forces and slip at the contact interface.

Friction and slip are crucial to dexterous manipulation with soft fingers [6], [7]. Consider the case of a cylinder, which cannot be stably grasped without friction. When a human picks up a cylindrical can of soda, the downward force of gravity is balanced by the upward tangential forces exerted by skin friction at the regions of contact. Likewise, skin friction makes it possible to hold a cylindrical pen during writing, and to exert torque while turning a knob. When friction is insufficient, the result is slip.

With soft fingers, slip is not an all-or-none process. Rather, it begins at the outer boundary of the contact region and then progresses inward [8], [9], [10]. During the initial phase of this process, known as incipient slip, the center of the contact region remains in static contact. If the process continues, then the entire contact region may slide and control of the grip may be lost. Humans can sense incipient slip and its progression towards full slip, and can adjust the contact force appropriately [11], [7]. Vibration due to surface microtexture is one cue, but even in its absence humans are sensitive to the changing spatial distribution of shear at the fingertips. It would be valuable for a robotic tactile sensor to measure this changing shear field as well.

Commercial tactile sensors fall short in various ways. They typically measure normal force or pressure, rather than shear; thus they ignore the critical tangential forces. Without measuring the shear field, and observing its change over time, it is difficult to determine incipient slip or total slip.

Another limitation typically found in tactile literature is that only discrete contact conditions, such as validation experiments on loads with point indenters, are considered. However, in the real case, the contact is a continuous surface with continuous distribution of stress and surface deformation. The continuity of the surface provides abundant information of the contact.

We have devised a soft fingertip that incorporates a novel tactile sensing system, allowing measurement of the changing patterns of shear over the contact region. The fingertip is a variant of the GelSight sensor that has been previously used in other tasks such as lump detection [12], texture classification [13], and alignment for insertion [14].

A GelSight sensor consists of a slab of clear elastomer covered with an opaque reflective membrane [1]. An embedded camera and light source measure the geometric properties of the membrane as it contacts surfaces. Prior GelSight sensors have mainly relied on photometric stereo to determine surface's 3D topography. We now extend the sensor to measure shear as well.

Soft tactile sensors with embedded cameras have been previously described. Hristu et al. [15] used a soft finger with a small number of markers and inferred the overall finger shape by fitting a parametric model. GelForce [16] used an array of embedded markers and showed how to infer the overall shear. Ito et al. [20] developed a dome-shaped soft tactile sensor with markers on the surface and use the markers to estimate the degree of slippage. These sensors applied various models in the measurement, but are mostly limited to specific contact conditions, such as some require point contact and others require contact with only flat surfaces parallel to the sensor surface. Our new GelSight sensor incorporates markers in the reflective membrane, patterned in a fairly dense quasi-random pattern. By measuring the displacement of the markers we can sample the elastomer's planar displacement at multiple locations, and thereby derive

[1]Department of Mechanical Engineering, and Computer Science and Artificial Intelligence Laboratory(CSAIL), MIT, Cambridge, MA 02139, USA `yuan_wz@csail.mit.edu`

[2]Department of Electrical Engineering and Computer Science (EECS) and CSAIL, MIT, Cambridge, MA 02139, USA `rui@csail.mit.edu`

[3]Laboratory for Human and Machine Haptics (MIT TouchLab), Research Laboratory of Electronics and Department of Mechanical Engineering, MIT, Cambridge, MA 02139, USA `srini@mit.edu`

[4]Department of Brain and Cognitive Sciences and CSAIL, MIT, Cambridge, MA 02139, USA `adelson@csail.mit.edu`

a displacement field. Combined with tracking the markers, the GelSight sensor is able to measure force and torque loads under a wider set of contact conditions in addition to its original capability to measure 3D geometry of the surface with high spatial resolution.

In this paper, Section II introduces the GelSight tactile sensor; Section III describes indentation experiments on the sensor loaded with normal force, shear force and torque. The states of shear, incipient slip, and slip states under shear are also discussed in detail. Section IV introduces several examples of using the sensor and an application of our tactile sensing method with an experimental setup to mimic a realistic scenario of grasping by a robot.

II. THE GELSIGHT SENSOR

The basic design of a GelSight sensor is introduced in [17], [1]. It consists of a piece of clear elastomer coated with a reflective membrane, along with a camera and light sources. When an object is pressed against the membrane, the membrane deforms to take the shape of the object's surface and the membrane deformation is recorded by a camera under illumination in different directions. The latest compact GelSight device, called the Fingertip GelSight sensor [14], is a small plastic cube with an elastomeric gel mounted on one side. LEDs of multiple colors send light through the light guiding plates toward the membrane, and a small camera captures the image of the membrane, which reflects the elastomer's deformation during contact. The softness of the elastomer and the reflectivity of the coating membrane influence the sensor's sensitivity to different sensing targets. In a typical design of the fingertip sensor, the transparent elastomer is made of the silicone rubber XP-565 from Silicones, Inc., with the neo-Hookean coefficient μ of 0.145MPa. Computer vision algorithms interpret the color image into the 3D topography of the touched surface. Fig. 1(a) shows a design of the Fingertip GelSight sensor, and Fig. 1(b) shows its schematic with different components illustrated. Fig. 1(c) shows the height maps obtained by the Fingertip GelSight sensor when contacting a human fingertip, where the brightness represents the amount of protrusion or height of the surface texture. Fig. 1(d) shows the fingertip sensor mounted on a robot gripper. On the Matlab platform with a personal computer, the whole system for recovering surface topography can run at over 10Hz for images of resolution 640x480, which allows its online use during robot tasks.

In this paper, we study the force interaction between the fingertip GelSight sensor and the contacting object. The interaction is inferred from the deformation of the elastomer. To track the elastomer's planar deformation, we added some specially designed markers on the elastomer's membrane, as shown in Fig. 1(e). The markers are triangular, and are scattered in a close to even but random way. The average distance between two adjacent markers is about 1.2 mm, and the average length of the markers is about 0.40 mm. The markers are sparse so that the GelSight's original function of getting the surface topography is only lightly disturbed. The GelSight camera takes images of the elastomer, as well
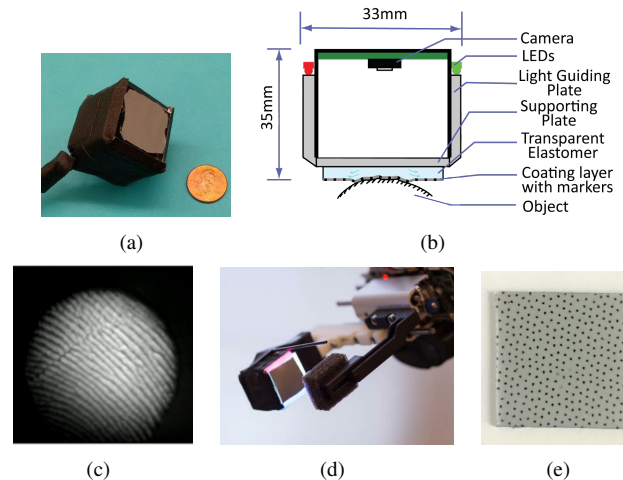

Fig. 1. (a) Fingertip GelSight sensor. (b) Schematic of Fingertip GelSight sensor. (c) Height maps obtained from Fingertip GelSight sensor when contacting human finger: brightness represents amount of protrusion of the surface. (d) A GelSight device mounted on a robot gripper. (e) Elastomer gel with markers

as the planar position of the markers, and the displacement of the markers is obtained by comparing the positions of the markers in different frames. The overall displacement field of the elastomer surface is obtained by interpolating the displacements of the markers, with a precision of 1.2 mm (the interval distance of the markers). The random sizes and distribution of the markers help in determining their location when measuring the displacement field. The density of the markers could be improved to obtain a displacement field of higher precision, but there is a tradeoff of the marker density and the GelSights function of measuring contact surfaces height map. The current density was chosen to achieve a good balance of keeping the two functions parallel.

III. INDENTATION EXPERIMENTS

To learn the GelSight sensor's response to different external loads, we designed an experimental setup to exert a variety of loads on the GelSight sensor under ideal conditions, as is shown in Fig. 2. The GelSight sensor contacts a replaceable rigid indenter, which is similar to contacting an external object's surface. Different sizes of indenters are used in the experiments, including flat-ended indenters and cylindrical indenters, to simulate contact with flat and curved surface. Three linear stage micrometer readers control the relative displacement between the indenter and the sensor in the normal direction, shear direction and the rotational direction, with linear precision of 0.01mm and rotational precision of $0.1°$. Therefore, the stages control the normal load, shear load and torsional load of the indenters on the GelSight sensor. An ATI Nano17 6-axis force/torque sensor is mounted before the indenter to precisely measure the resultant force and torque during the contact. The elastomer sensor used in this experiment is a square sheet measuring 23.4mm×22.6mm×2.0mm, and the the camera's field of view is 17.67mm×13.25mm.
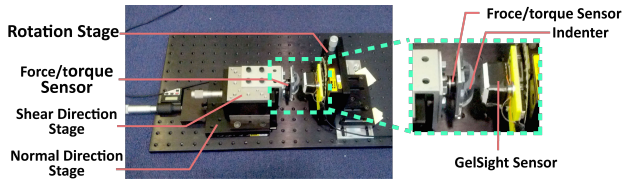
Fig. 2. The setup for indentation experiments.

A. Displacement fields under Loads

The displacement field of the GelSight markers is determined by the load on the contact surface. The loads used for the experiments described in this paper include the normal, shear and torque loads. Different loads cause different patterns on the marker displacement field, and thus serve as features of the loads. The displacement magnitude increases as the load increases.

The normal load is the force load in the normal direction to the contact surface. In a robotic grasp work, the normal force is the squeezing force when holding an object. Under the normal force, the elastomer on the GelSight sensor is squeezed sideways from the contact center, so that the displacement field is in a pattern of spreading outwards from the contact center, as is shown in Fig. 3. According to [18] and the finite element simulation results [19], when contacting a flat surface in the parallel direction, the indenting depth is homogeneous, and the pressure grows higher in the border area; when the contact surface is not flat and the indenting depth is not homogeneous, the pressure concentrates in the more deeply indented area, and the displacement field mainly spreads from the deeply indented area to the lightly indented area, as shown in the cylinder indenter case in Fig. 3(c). The overall displacement magnitude is in positive correlation to the normal force. When the load is not large, the indenting depth, normal force, and magnitude of the displacement field are all in linear relationship under the same indenter.
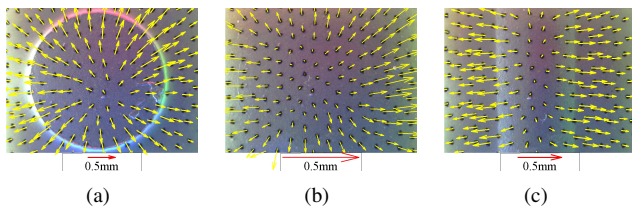

Fig. 3. Displacement fields for normal indentation with different indenters. (a) Under a small flat-ended circular indenter with a diameter of 12.5mm; (b) Under a large flat-ended indenter that is in full contact with the sensor; (c) Under a cylinder indenter with a diameter of 38.08mm.

The shear force is the contact force in the tangential direction to the contact surface. The contact shear force is commonly seen in robotic scenarios, especially in grasping tasks. The force of gravity on the object causes downward shear force on the contact surface. Measuring the shear force can be used to estimate the object's weight and judge whether the object is likely to slip. The displacement field pattern under shear load is homogeneous and all to the shear

direction within the contact area; in the non-contact area, the elastomer surface displacement due to the shear load quickly decreases to zero. The overall displacement magnitude is in positive relation to the shear force. Fig. 4 shows the displacement field caused by shear loads under the large flat-ended indenter. Fig. 4(a) is the displacement field under a small shear load and Fig. 4(b) is the displacement field under a large shear load, where the displacement magnitude is larger and inhomogeneity grows due to the occurrence of partial slip. The relationship between shear load, partial slip and total slip is further introduced in Section III-B.
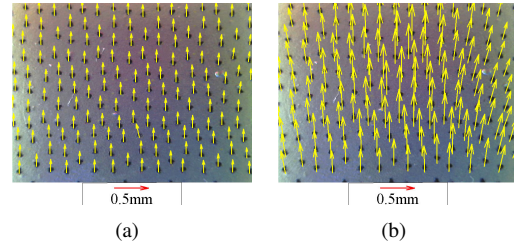

Fig. 4. The displacement field for pure shear under (a) a 0.2mm's displacement shear load and (b) a 0.7mm's displacement shear load. When the load is small, the shear displacement field on contact surface is homogenous and in the shear direction; when the load is large, the field is inhomogeneous and directions diverge.

During a single shear loading process, the average displacement of the markers is found to be proportional to the shear force. Fig. 5 and Fig. 6 show the change of the markers' average shear displacement with the measured shear force during a single shear indentation experiment with the large flat-ended indenter. Fig. 5 shows the result in quasi-static cases, and Fig. 6 in the non-equilibrated states when the shear force gradually decreases due to the occurrence of partial slip. However, the average marker displacements are all proportional to the shear force, and consequently it can serve as a measurement of shear force. More experiments with random shaped contact surfaces and contact conditions are planned to be conducted to verify this conclusion in more realistic contact situations.
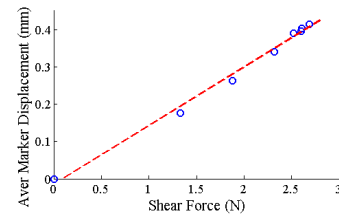

Fig. 5. Relationship of the average marker displacements and shear force. All in quasi-static states under the large flat-ended indenter. The shear force is proportional to the average shear displacement of the elastomer over the contact area.

The torsional load studied in this paper refers to the load caused by the indenters rotation on the axis normal to the contact surface, or in-plane torsional load for short. The in-plane torsional load field is commonly seen when there is an external acentric load on the grasped object, or when the robotic grippers grflatasping points on the object do not align
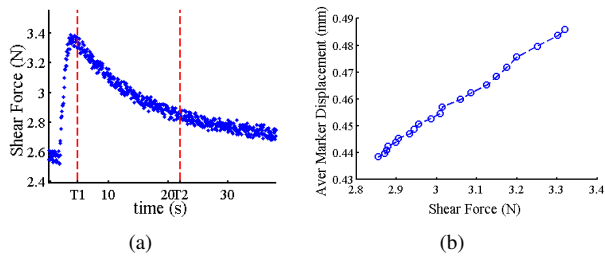
Fig. 6. Change of shear force and markers' average shear displacement during a non-equilibrated period. (a) Shear force change after a step increase of shear load, when partial slip occurs. (b) Change of markers' average shear displacement according to the temporal shear force from T1 to T2 in (a). The figure shows that even during the non-equilibrium period the average shear displacement of the elastomer is still linearly related to the shear force.

with the axis through the objects center of gravity, causing a rotational slip to occur when the load is too large. Under the in-plane torsional load, the elastomer's displacement field is a spiral pattern. Fig. 7 shows an example of the displacement field caused by torsional load with the large flat-ended indenter. The displacement magnitude is also in positive relation to the torque applied.
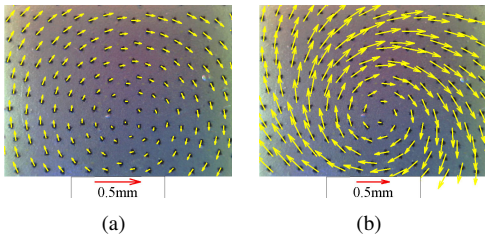

Fig. 7. Displacement field of large flat-ended indenter after different indenter's rotation of (a) 0.6 degree and (b) 4.5 degree

B. Shear Loading

Shear load is the force in the tangential direction on the contact surface. For a robot, the shear load is commonly seen in grasp tasks, where the object weight causes the shear load on the contact surface, and the shear contact state is crucial in deciding whether a grasp is firm enough or the object will fall. The shear force is also important for a robot to perceive the external force acting on the contact object, or to explore the friction on the contact surface.

An important problem for shear measurement is the occurrence of slip and incipient slip. During grasp, the occurrence of total slip indicates a grasp failure and the object slips away from the gripper. Incipient slip, which means slip is about to occur, is also of great research interest for preventing slip and grasp failures. The occurrence of slip is a fuzzy process and no obvious boundary exists. The states under shear load can be nominally divided into the shear state, the partial slip state and the slip state according to the relative displacement between the indenter and the elastomer: (1) The shear state: when load is small and no relative movement occurs between the indenter and the elastomer; (2) The partial slip state: when the load is larger and relative movement occurs in part of the contact region; (3) The slip state: when the load is very

large and there is relative movement over the whole contact region. When the partial slip is serious and the relative moving contact area is large enough, slip is likely to occur soon, and the state is considered incipient slip. However the boundary for incipient slip is more ambiguous.

In the shear indentation experiments we mainly studied the displacement field patterns of quasi-static states. The time-dependent response of the elastomer's displacement field is introduced later in this section. To make the quasi-static contact condition, the experimental setup shown in Fig. 2 firstly exert a normal load towards the GelSight sensor, and the normal load remains through the whole process. Then the linear stage moves the indenter in the upward direction to exert a shear load. The indenter moves in steps, and there is a long enough period (around 3 minutes) of waiting at each step for the elastomer to reach a quasi-static state. The indenters used are a large flat-ended indenter that is in full contact with the sensor and a cylinder indenter with the diameter of 38.08mm. They are two representatives for the contact of a flat surface and a curved surface. When using the large flat-ended indenter, the relation between the shear force and the indenter's shear displacement is shown in Fig. 8. The shear force is measured by the force/torque sensor in the experimental setup.
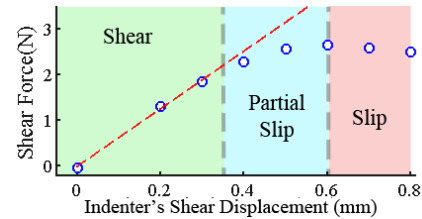

Fig. 8. Relationship between shear force and indenter's shear displacement in quasi-static states. During shear state, shear force is proportional to the indenter displacement; during partial slip state, shear force increases more slowly; during slip state, shear force does not increase.

In Fig. 8, the approximate boundary of states of shear, partial slip and slip are determined according to the relative displacement between the indenter and the elastomer. As is shown, during the shear state the shear force is in linear relationship to the indenter's shear displacement; during the partial slip state, the shear force grows as the shear displacement grows but slower than the linear fit; during the slip state, the shear force does not grow and even decreases slightly. The magnitude of the displacement field can be used to infer the states of shear, partial slip and slip. Fig. 9 shows the interpolated difference distribution between the indenter's shear displacement and the elastomer's displacement in the shear direction. The dark blue area is the place that the elastomer displacement is close to the indenter's displacement, and red area indicates there is a large difference between the indenter's displacement and the elastomer's displacement, i.e. partial slip occurs. Fig. 9(a) shows the magnitude difference during the shear state, where the displacement magnitude is very homogeneous; Fig. 9(b) shows the magnitude difference during the partial slip period and the displacement field

magnitude is not so homogeneous as the previous case, and the distribution indicates partial slip occurs from the contact border; Fig. 9(c) shows the case when the partial slip is more serious, and the inhomogeneity grows; Fig. 9(d) shows the case when the load is large and total slip occurs. The inhomogeneity of the displacement field magnitude is similar to Fig. 9(c), but there is no blue area in the figure, which means slip occurs in the whole area.

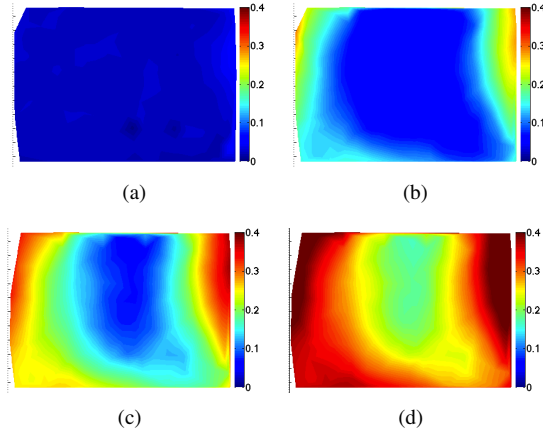(a)   (b)

(c)   (d)

Fig. 9. Difference distribution of indenter's shear displacement and elastomer's displacement, under the load shear displacement of (a) 0.20mm (shear state), (b) 0.50mm (partial slip state), (c)0.60mm (partial slip state) and (d) 0.70mm (slip). Color axis scale in mm. Blue area means little local slip occurring. As the load increases, the inhomogeneity of displacement field magnitude increases, which indicates a increasing degree of partial slip and likelihood of slip occurring.

Fig. 10 shows a plot of the indenter's shear displacement against the maximum marker displacement, which is also the maximum displacement on the elastomer's surface. When the indenter's displacement is equal to or smaller than 0.6mm, no overall slip occurs, and the maximum marker displacement is close to the displacement of the indenter; at higher values of indenters shear displacement, total slip occurs, and the maximum marker displacement remains or even slightly decreases.
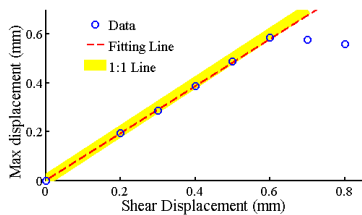

Fig. 10. Relationship of max marker displacement and indenter's shear displacement in quasi-static states.

As shown in the experiment, the inhomogeneity of the displacement field magnitude shows the degree of partial slip or slip quite well, and can be considered as a measure to indicate the likelihood of slip to occur. There are multiple statistical ways to quantitively describe the inhomogeneity of the field, and one measurement is the entropy of the field. The entropy here is a statistical measure of the randomness

of a histogram. The entropy of a histogram X is

$$H(X) = - \int_X p(x) \log p(x) dx,$$

and a smaller entropy indicates a more concentrated distribution of the histogram. In this paper, the histogram X is obtained from the displacement field magnitude tensity, and $p(x)$ refers to the distribution. In the shear experiment with the large flat-ended indenter, the entropy of the shear field magnitude under increasing shear displacement is shown in Fig. 11. The boundaries of shear, partial slip and slip are the same as those in Fig. 8. The entropy grows as the partial slip degree grows, and can be seen clearly differentiate each of the three states.
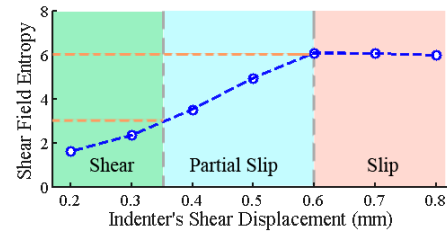

Fig. 11. Entropy of the shear displacement field magnitude under different loads with the large flat-ended indenter. The value indicates the inhomogeneity of displacement field, which predicts the degree of partial slip.

Typically it is hard to precisely define a boundary for slip occurrence or the incipient slip state. For the sake of robotic manipulation, we can set a rough boundary where we consider the partial slip is severe enough and slip is likely to happen soon. For example, in the large flat-ended indenter case, we can consider the entropy area 4.5 − 6 is the "incipient slip" state, and if the entropy of the GelSight displacement field reaches this area during a robotic grasp, then the robot must take some action to secure the grasp.

There is a hysteresis in the elastomer's response to an external load, mostly influenced by the viscosity of the material. Therefore, during the load process, it takes some time for the elastomer displacement field to reach a quasi-static state. Fig. 12 shows the elastomers temporal response after a step increase of indenter displacement in the shear direction. Fig. 12(a) shows the change of shear force during the process: in T1 to T2, a rapid growth due to the indenter's step displacement; after T2, the shear force decreases, and it reaches a quasi-static state after about 3 minutes. Fig. 12(b) to (d) shows the elastomer displacement fields at different times. During the step load increase period, the elastomer surface displaces homogeneously in the shear direction; after the load reaches its maximum, the central part of the contact area remains static, and the peripheral area partially slips back. Most of the slip occurs soon after the load stops increasing, in the T2 to T3 period, which is also the period when the shear force decreases most rapidly. In the T3 to T4 period, the shear force decreases very slowly and finally researches a quasi-static state, and the elastomer surface displaces very little.
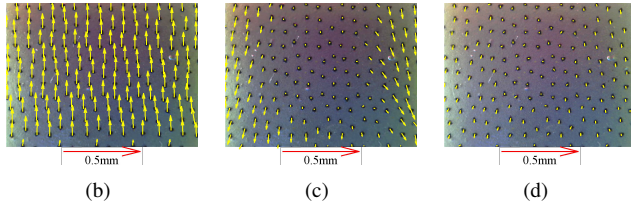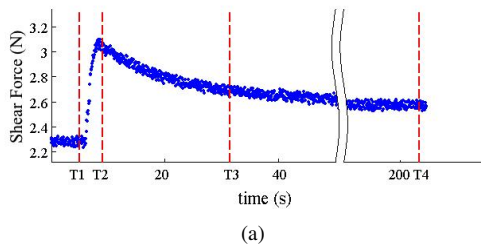
Fig. 12. An example of temporal change sequence after a step shear load increase, where partial slip originates in peripheral contact region, and most partial slip happens in a short period after load increase, as simultaneously shear force rapidly drops. (a) Shear force change after step increase of load. Elastomer displacement (b) from T1 toT2, (c) from T2 to T3, and (d) from T3 toT4.

When the step change in the indenter shear displacement is large, total slip occurs immediately, and the final quasi-static shear force is close to the shear force before the step displacement. During the step loading, the shear force increases rapidly, and the displacement field is also homogeneous. Total slip occurs quickly after the loading, which is accompanied by a sharp decrease in the shear force and the moving back of the displacement field. In contrast, no slip occurs at all after the step displacement when it is small, and the shear force barely decreases after the step loading and the displacement field remains unchanged.

We also conducted another shear experiment with the cylinder indenter to measure the shear displacement field when the contact surface is not flat. The cylinder indenter has a diameter of 38.08mm and is firstly pressed to the GelSight's elastomer surface on the side. Then the indenter is moved in the upward direction to exert a shear load, which is along the length of the cylinder. The scenario is very similar to the case of a robot hand lifting a cylindrical object like a soda can, although in this case the shear force is applied downwards due to gravity. The elastomer's response to the shear load of the cylinder indenter is very similar to that of the flat-ended indenter.

The displacement fields caused by a cylinder indenters shear load is shown in Fig. 13, and they are similar to the displacement fields of the large flat-ended indenter. When the load is small and within the shear state, the elastomers displacement magnitude within the contact area is homogenous and all towards the shear direction; when the load is larger, partial slip occurs and finally slip occurs, accompanied by the growth of inhomogeneity of the displacement magnitude. Partial slip also begins from the border of the contact area. For the contact of a cylinder, the normal pressure is much larger in the middle area because of the higher indentation
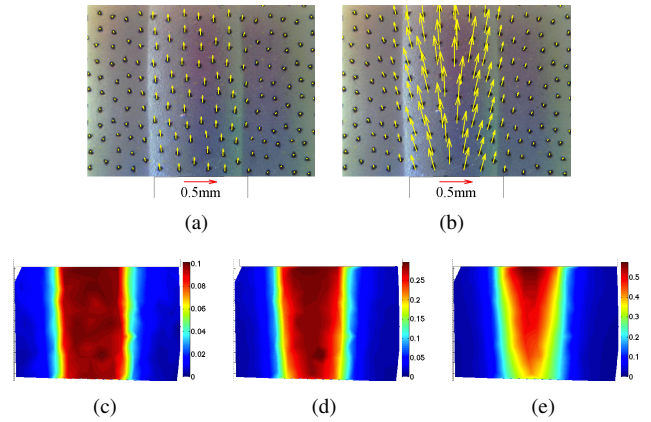

Fig. 13. Shear displacement fields for a cylinder indenter. The vector fields under (a) 0.1mm's displacement load and (b) 0.6mm's displacement load. (c), (d), and (e) are displacement field magnitudes under different shear load. Color map's axis unit in mm. Similar to flat-ended indenter cases, as load increases and degree of partial slip increases, inhomogeneity of shear field magnitude increases.

depth there. Therefore, partial slip occurs more easily at the contact border, and there is a larger range for incipient slip. The resultant contact shear force is also in linear relationship to the sum of local displacements in the shear direction.
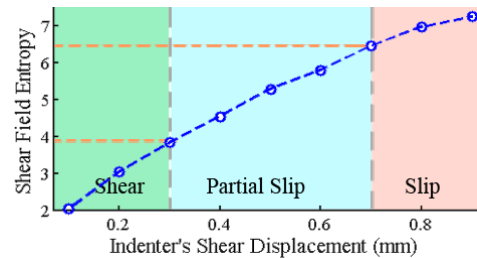

Fig. 14. Entropy of the shear displacement field magnitude when loaded by the cylinder indenter. The value is related to degree of partial slip.

The entropy of the displacement magnitude in contact area versus different shear loads is shown in Fig. 14. The contact area is calculated according to the heightmap by the GelSight sensor [17]. The entropy also increases as the shear load and the partial slip degree increases, but it differs compared to the entropy of the flat-ended indenter, because of the differences in the surface geometry. In the shear case with the cylinder indenter, the entropy of partial slip state is roughly between 4 to 6.5, and in the practical cases we can suppose the entropy between 5–6.5 is the "dangerous area" and slip is likely to occur soon as the load increases.

IV. GRASPING EXPERIMENTS

We built a mechanical jig to simulate the grasp of a two-finger robotic gripper, and installed the GelSight sensor on it to see the response of the sensor during interaction with the object. We studied different kinds of loads. The equipment is shown in Fig. 15(a), with two overhang holders to hold the object. There are two rails on the jig to control the clamping and lifting of the holder, simulating the grasping and lifting process with a robot gripper.
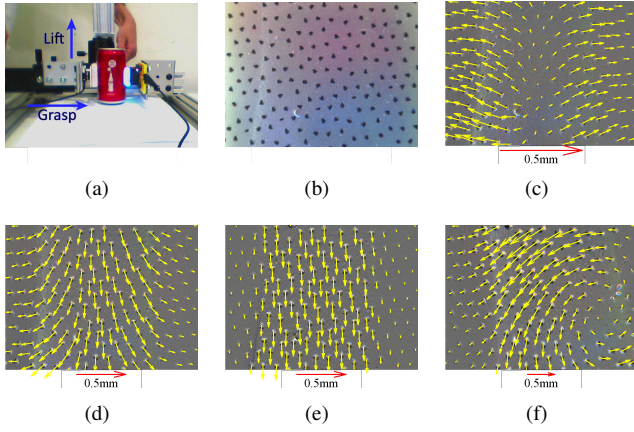
Fig. 15. A grasping experiment with a soda can. (b): GelSight camera view during grasp; (c): displacement field when grasping stably; (d): displacement field when the can is lifted stably, with shear field shown in (e) after subtracting the normal load displacement field of (c). (f) shows the response to an external torque on the can.

Fig. 15 shows the results when grasping a soda can. The can is cylindrical with a smooth surface. When the gripper holds the can stably, the displacement field of the GelSight elastomer surface is static, as shown in Fig. 15(c), which is very similar to the displacement field of the normal indentation experiment with the cylinder indenter. Some small deviation exists on the displacement field due to the small friction during the contact, which is very common for most grasping tasks. When lifting the can at a slow speed or holding it in the air, the displacement field is stable, and there is a stable vertical shear force due to gravity. The shear field is shown in Fig. 15(e) after subtracting the field of normal contact. Fig. 15(f) shows the response of the elastomer displacement when the can is shaken back and forth, such that an external torque is applied.
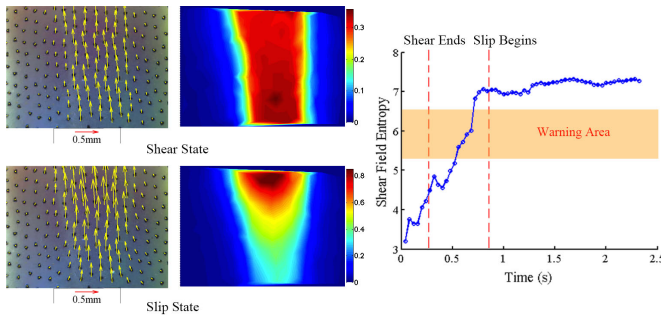

Fig. 16. The change of shear displacement field entropy as the soda can is pulled from the gripper. Left figures show the shear displacement field and the magnitude of the field during shear and slip states. The orange range on the entropy plot indicates incipient slip states.

Fig. 16 shows an experiment in which the soda can held in the gripper is pulled away by a human. A human pulls the soda can away by increasing the upward force, and the contact states of the gripper and the soda are shear, partial slip, and slip as time goes on. The shear displacement

field and the magnitude distribution are shown on the left. Similar to the indentation experiment, during shear state the displacement field is homogenous, and in the slip state the field is much more inhomogeneous. The contact area is estimated through the GelSight's hight map. The field's entropy is shown in the right part of the figure, which grows with time as partial slip increases and slip occurs. The orange area is the potentially dangerous area of the incipient slip, and we expect the real robot to take some precaution during that period to prevent the potential slip occurrence. The range of the warning area is estimated from the shear experiment with the cylinder indenter and the results in Fig. 14.
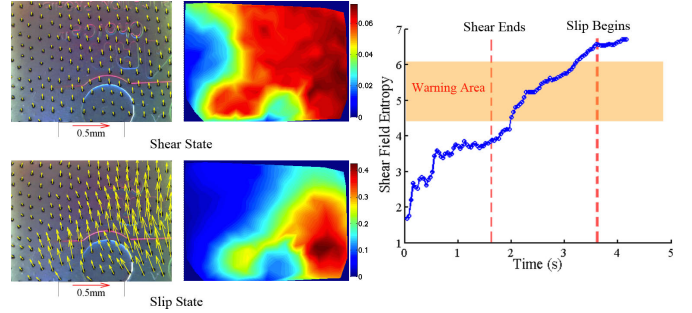

Fig. 17. The change of shear displacement field entropy as a held key is pulled from the gripper. Left figures show the shear displacement field and the magnitude of the field during shear and slip states. The orange range on the entropy plot indicates incipient slip states.

We also ran grasping experiments on other objects like pens, keys, spoons, and USB plugs, and they confirmed that the displacement field of the surface markers effectively represent the contact condition of the sensor and the object. An experiment of pulling a key from the gripper is shown in Fig. 17, with the key having a flat-shaped surface with complicated emboss. The displacement field shows similar properties as with other regular objects, and the entropy of the field well indicates of the likelihood of slip quite well. The warning area for incipient slip in this experiment is estimated from the shear experiment with the flat-ended indenter and the results in Fig. 11.

V. DISCUSSION

To summarize, with the tracking-surface-marker method, the displacement field of the GelSights elastomer surface reflects the external load at the contact surface, and it effectively indicates the degree of partial slip during the shear loading. The inhomogeneity degree of the displacement magnitude within the contact area matches the degree of partial slip, and entropy is one quantitive measure of the inhomogeneity of the field. A range of entropy values can be determined beyond which we can predict that slip will occur soon. Based on the current data, we find that the entropy is lightly influenced by the geometry of the contact surface. Measuring shear and the incipient slip during contact with objects is important for robot tasks, especially grasp, in that the warning of incipient slip helps to prevent grasp failure.

Obtaining a quantitative measurement of the force or torque with a tactile sensor using deformable polymer as the contact medium can be complicated due to the non-linearity and hysteresis response of the material. Surprisingly in our experiments, the average displacement of the elastomer markers was found to be proportional to the overall shear force in both quasi-static states and non-equilibrated states, regardless of the occurrence of partial slip or total slip, which shows promise in the use of the tracking-marker method to measure shear force. In fact, the local marker displacement due to the shear load is more likely to reflect the local shear stress. More experiments to verify the sensors performance under different indenters and normal pressures are to be conducted for a more robust conclusion.

In this paper, we have focused on measuring the degree of partial slip and providing a warning before slip occurs, as we think they are important to robot contact tasks. However, to exactly measure the slip occurrence, the current tracking-marker method may need to include comparison of the marker displacement and the movement of the object from the GelSights height map

VI. CONCLUSIONS

In this paper, we have proposed a method of inferring the contact loads and slip on the GelSight sensor. The GelSight sensor is an optical-based tactile sensor that uses a piece of elastomer as the contact medium and reconstructs the 3D topography of the contact surface according to the deformation of the elastomer surface. In this paper, we focused on tracking the planar deformation field of the elastomers membrane by tracking the movement of patterned markers on the elastomer's surface, thus obtaining more information about the contact condition. The displacement field has distinct responses to the normal load, shear load and in-plane torsional load respectively, with the displacement magnitude in positive correlation to the load. The displacement distribution is a good indicator of the degree of partial slip under the shear load, as measured by its inhomogeneity in displacement magnitude, which can be quantified by the entropy of the field. This information can help a robot to perceive physical interactions with the external environment, and can serve as an important guide for robot manipulation. Detecting incipient slip can help a robot to exert control to prevent grasp failure. We conducted experiments on a gripper-like mechanical jig and successfully demonstrated that the method works in practice. Finding a way to apply the tracking-marker method in the real operations scenarios is another challenge to be solved in the future. The load is much more complicated in the real cases, and the load on the contact surface is usually a combination of different kinds of forces and torques. Although each of the forces and torques result in their own specific displacement fields, it remains difficult to decompose the resultant displacement field into component fields caused by the different load components. GelSight's ability to estimate the height map of the contact surface will be helpful in the process.

REFERENCES

[1] M. K. Johnson, F. Cole, A. Raj, and E. H. Adelson, "Microgeometry capture using an elastomeric sensor," in *ACM Transactions on Graphics (TOG)*, vol. 30, no. 4. ACM, 2011, p. 46.

[2] R. S. Dahiya, G. Metta, M. Valle, and G. Sandini, "Tactile sensingfrom humans to humanoids," *Robotics, IEEE Transactions on*, vol. 26, no. 1, pp. 1–20, 2010.

[3] H. Yousef, M. Boukallel, and K. Althoefer, "Tactile sensing for dexterous in-hand manipulation in roboticsa review," *Sensors and Actuators A: physical*, vol. 167, no. 2, pp. 171–187, 2011.

[4] (2014) Tactarray instrumentation solutions – pressure profile systems. [Online]. Available: http://www.pressureprofile.com/tact-array-sensors

[5] N. Wettels, J. Fishel, Z. Su, C. Lin, and G. Loeb, "Multi-modal synergistic tactile sensing," in *Tactile sensing in humanoidsTactile sensors and beyond workshop, 9th IEEE-RAS international conference on humanoid robots*, 2009.

[6] R. D. Howe, I. Kao, and M. R. Cutkosky, "The sliding of robot fingers under combined torsion and shear loading," in *Robotics and Automation, 1988. Proceedings., 1988 IEEE International Conference on*. IEEE, 1988, pp. 103–105.

[7] M. A. Srinivasan, J. Whitehouse, and R. H. LaMotte, "Tactile detection of slip: surface microgeometry and peripheral neural codes," *Journal of Neurophysiology*, vol. 63, no. 6, pp. 1323–1332, 1990.

[8] J.-s. Chen and M. A. Srinivasan, "Human haptic interaction with soft objects: discriminability, force control, and contact visualization," MIT, Cambridge, MA, Touch Lab Report 7 RLE TR-619, 1998.

[9] J. C. Liao and M. A. Srinivasan, "Experimental investigation of frictional properties of the human fingerpad," Touch Lab Report 11, MIT, Cambridge, MA, Tech. Rep. RLE TR-629, Aug. 1999.

[10] M. J. Adams, S. A. Johnson, P. Lefvre, V. Lvesque, V. Hayward, T. Andr, and J.-L. Thonnard, "Finger pad friction and its role in grip and touch," *Journal of The Royal Society Interface*, vol. 10, no. 80, 2013.

[11] R. Johansson and G. Westling, "Roles of glabrous skin receptors and sensorimotor memory in automatic control of precision grip when lifting rougher or more slippery objects," *Experimental Brain Research*, vol. 56, no. 3, pp. 550–564, 1984.

[12] X. Jia, R. Li, M. A. Srinivasan, and E. H. Adelson, "Lump detection with a gelsight sensor," in *World Haptics Conference (WHC), 2013*. IEEE, 2013, pp. 175–179.

[13] R. Li and E. H. Adelson, "Sensing and recognizing surface textures using a gelsight sensor," in *Computer Vision and Pattern Recognition (CVPR), 2013 IEEE Conference on*. IEEE, 2013, pp. 1241–1247.

[14] R. Li, R. Platt Jr, W. Yuan, A. t. Pas, N. Roscup, M. A. Srinivasan, and E. H. Adelson, "Localization and manipulation of small parts using gelsight tactile sensing," 2014.

[15] D. Hristu, N. Ferrier, and R. W. Brockett, "The performance of a deformable-membrane tactile sensor: basic results on geometrically-defined tasks," in *Robotics and Automation, 2000. Proceedings. ICRA'00. IEEE International Conference on*, vol. 1. IEEE, 2000, pp. 508–513.

[16] K. Sato, K. Kamiyama, N. Kawakami, and S. Tachi, "Finger-shaped GelForce: sensor for measuring surface traction fields for robotic hand," *IEEE Transactions on Haptics*, vol. 3, no. 1, pp. 37–47, Jan. 2010.

[17] M. Johnson and E. Adelson, "Retrographic sensing for the measurement of surface texture and shape," in *Computer Vision and Pattern Recognition, 2009. CVPR 2009. IEEE Conference on*. IEEE, June 2009, pp. 1070–1077.

[18] K. L. Johnson, *Contact mechanics*. Cambridge university press, 1987.

[19] W. Yuan, "Tactile measurement with a gelsight sensor," Master's thesis, MIT, Cambridge, MA, USA, 2014.

[20] Y. Ito, Y. Kim, and G. Obinata, "Robust slippage degree estimation based on reference update of vision-based tactile sensor," *Sensors Journal, IEEE*, vol. 11, no. 9, pp. 2037–2047, 2011.